ACS APPLIED MATERIALS & INTERFACES

Research Article

www.acsami.org

Liquid Exfoliated Graphene as Dopant for Improving the Thermoelectric Power Factor of Conductive PEDOT:PSS Nanofilm with Hydrazine Treatment

Jinhua Xiong,† Fengxing Jiang,† Hui Shi, Jingkun Xu,* Congcong Liu, Weiqiang Zhou, Qinglin Jiang, Zhengyou Zhu, and Yongjing Hu

Department of Physics, Jiangxi Science and Technology Normal University, Nanchang 330013, China

Supporting Information

ABSTRACT: Here, we fabricated a highly conductive poly(3,4-ethylenedioxythiophene):poly(4-styrenesulfonate) (PEDOT:PSS) nanofilm via vacuum filtration with enhanced thermoelectric power factor by doping of liquid exfoliated graphene (GE) and hydrazine treatment. The effect of GE exfoliated in dimethylformamide (DMF) and *N*-methyl-2-pyrrolidone (NMP) on the electrical conductivity and thermopower of PEDOT:PSS was investigated. Although electrical conductivity decreased with increasing GE, thermoelectric power factors of PEDOT:PSS nanofilms were improved with 3 wt % GE in DMF (38.6 μW m^{-1} K^{-2}) and in NMP (28.0 μW m^{-1} K^{-2}) compared to pure PEDOT:PSS (11.5 μW m^{-1} K^{-2}). The mechanism of improvement was proposed to be the removal of PSS and the good interaction between PEDOT and GE. With hydrazine treatment, 3 wt % GE-doped PEDOT:PSS nanofilm (PG3) showed a further enhanced power factor of 53.3 μW m^{-1} K^{-2} (~5 times higher than that of pristine PEDOT:PSS nanofilm). The effects of hydrazine containing concentration, treatment time, and temperature on the electrical conductivity and Seebeck coefficient of PG3 were investigated systematically. An estimated thermoelectric figure of merit (ZT) is 0.05 with the optimized power factor at room temperature.

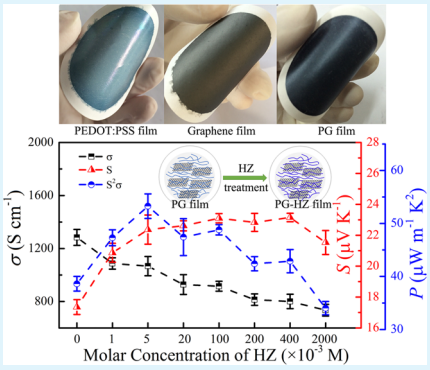

KEYWORDS: *PEDOT:PSS, exfoliated graphene, nanocomposite, power factor, hydrazine treatment*

1. INTRODUCTION

The field of organic materials has been intensively investigated in the past decade because of its potential thermoelectric (TE) property.[1,2] The TE property is generally determined by a dimensionless figure of merit, $ZT = \sigma S^2 T/\kappa$, where σ, S, κ, and T are the electrical conductivity, the Seebeck coefficient, the thermal conductivity, and the absolute temperature, respectively. A good TE material requires a large power factor ($P = \sigma S^2$) and a low thermal conductivity. Compared to inorganic materials, organic materials possess several advantages as TE materials, such as low thermal conductivity, cost-effectiveness, mass production, facile synthesis, and wide area processing.[3,4] However, a main challenge for organic TE materials is to achieve simultaneously a high electrical conductivity and a large Seebeck coefficient. High TE power factors of organic materials are expected due to their intrinsic advantages.[5,6]

Poly(3,4-ethylenedioxythiophene):poly(4-styrenesulfonate) (PEDOT:PSS) is one of the most excellent conducting polymers due to its water solubility, mechanical flexibility, low cost, and commercial availability.[7−9] Furthermore, PEDOT:PSS is a promising candidate as an organic TE material because of its high electrical conductivity through secondary treatment. In conventional semiconductors, increasing electrical conductivity, if induced by an increasing carrier concentration, usually results in a decrease of Seebeck coefficient, which restrains the improvement of the power factor.[10] Surprisingly, the enhanced electrical conductivity does not lead to a decreasing Seebeck coefficient of PEODT:PSS.[11] Kim et al. obtained a high electrical conductivity (900−1000 S cm^{-1}) of PEDOT:PSS by ethylene glycol (EG) and dimethyl sulfoxide (DMSO) posttreatment.[1] Xia et al. reported that the electrical conductivity of PEDOT:PSS can be enhanced to over 3000 S cm^{-1} by sulfuric acid treatment.[12] Nevertheless, highly conductive PEDOT:PSS suffers from a low Seebeck coefficient, which is generally measured in the 14−18 μV K^{-1} range.[13,14] Polymer−inorganic nanocomposites provide a promising way to improve the TE property. Most recently, PEDOT:PSS/inorganic TE materials have been reported by several groups in order to improve the Seebeck coefficient. Zhang et al. fabricated PEDOT:PSS/Bi_2Te_3 layer composite films by dropping PEDOT:PSS on top of a Bi_2Te_3 layer with a Seebeck coefficient of 110 μV K^{-1}.[15] Park et al. prepared PEDOT:PSS/Ge composite films by drop-casting with an optimized Seebeck coefficient of 58.9 μV K^{-1}.[16] Presently, the TE property of organic composites focus on PEDOT:PSS/carbon nanotubes[17−20] and PEDOT:PSS/graphene.[21−23]

Received: April 28, 2015
Accepted: June 19, 2015
Published: June 19, 2015

DOI: 10.1021/acsami.5b03692
ACS Appl. Mater. Interfaces 2015, 7, 14917−14925

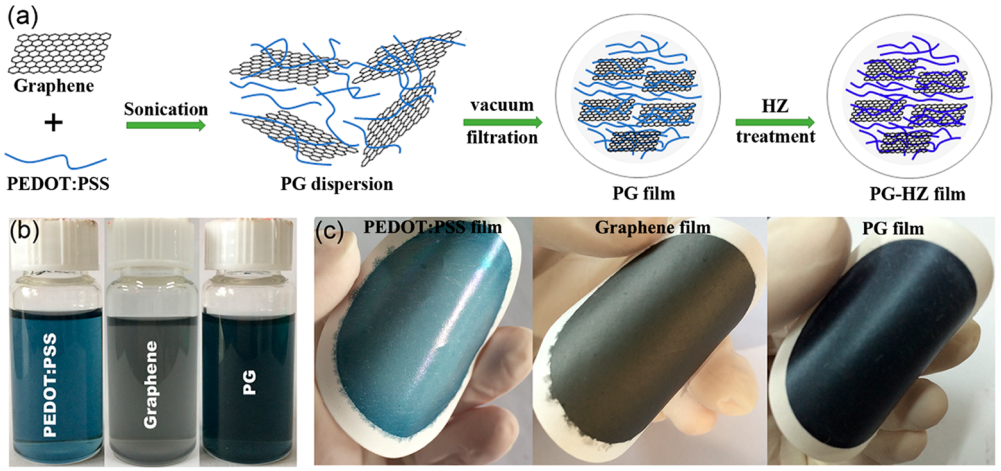

Figure 1. (a) Schematic illustration showing the preparation and HZ-treatment process of the PG nanofilm. (b) Photographs of a dispersion of PEDOT:PSS, graphene, and PG in DMF after sonication. (c) Photographs of PEDOT:PSS, graphene, and PG films.

Graphene, a monolayer of graphite, has attracted intensive interest as a promising TE material in recent years due to its unique two-dimensional (2D) structure, high electrical conductivity (160 S cm^{-1}),[24] and high carrier mobility (200000 cm^2 V^{-1} s^{-1}).[25] Moreover, graphene is simple in preparation method. Exfoliation is one of the most common methods, which can be achieved by overcoming the attractive van der Waals interactions between layers in graphite with the assistance of organic solvents, surfactants, polymers, and so on.[26−29] For the thermoelectric performance, Ni et al. obtained a maximum Seebeck coefficient of 600 μV K^{-1} and ZT of 5.8 for graphene strips by using density functional theory calculations combined with nonequilibrium Green's function method.[30] Moreover, previous experimental results showed that exfoliated single-layer and bilayer graphene showed a high Seebeck coefficient of 50−100 μV K^{-1}.[31−33] However, the exceedingly high thermal conductivity of graphene (2500−5300 W m^{-1} K^{-1})[34,35] makes it a poor contestant for TE property. An effective method is to combine a low thermal conductivity material with high electrical conductivity.[19]

The combination of PEDOT:PSS and graphene has been demonstrated to be a good choice for improving the electrical and thermal properties.[21] PEDOT:PSS/graphene (PG) nanocomposite materials have previously been studied as the basis of such as electrocatalyst, sensors, batteries, and supercapacitors and begun attracting considerable attention as TE materials recently.[36,37] The strong interaction between PEDOT:PSS and graphene with a rich conjugated system can effectively improve the electron transport property and the stability of materials.[38] Recently, most effort for the TE property of PEDOT:PSS/graphene has been concentrated in the combination of PEDOT:PSS and reduced oxide graphene (rGO). Kim et al. prepared PEDOT:PSS/rGO composite nanofilms through direct mixing of PEDOT:PSS and graphene by solution spin coating method and obtained a maximum power factor of 11.09 μW m^{-1} K^{-2} from a sample with 2 wt % rGO.[21] Li et al. fabricated a PEDOT:PSS/rGO composite using a simple wet-chemical route and exhibited a maximum power factor of 32.6 μW m^{-1} K^{-2}.[22] Yoo et al. prepared PEDOT:PSS/rGO composite films via an in situ polymerization method and exhibited enhanced TE property at room temperature (RT) with a power factor of 45.7 μW m^{-1} K^{-2}.[23] Nevertheless, the preceding research studies do not full synergistically combine the advantages of PEDOT:PSS and graphene because of the structural defects of rGO. Compared to rGO, exfoliated graphene has less structure defect and a higher electrical conductivity.[39,40] However, there are few reports on utilizing exfoliated graphene in TE materials as a composite additive.

In this work, we fabricated liquid exfoliated graphene doped PEDOT:PSS nanofilms by vacuum filtration and investigated their TE properties. The liquid exfoliated graphene showed a positive effect on the TE power factor of PEDOT:PSS. Considering the positive effect of solvents on the electrical conductivity of PEDOT:PSS,[41] the NMP and DMF were chosen as the dispersed solution of graphene. Hydrazine treatment for PG nanofilms was used to improve the TE power factor further. The effect of concentration, treatment time, and temperature of hydrazine on the electrical conductivity and Seebeck of PG was investigated. An improved TE power factor was found for PG nanofilm with hydrazine treatment optimization.

2. EXPERIMENTAL SECTION

2.1. Materials. PEDOT:PSS aqueous solution (Clevios PH 1000) was purchased from HC Stark (Munich, Germany). Graphite powder, dimethylformamide (DMF), *N*-methyl-2-pyrrolidone (NMP), and hydrazine (HZ, 80 wt % aqueous solution) were purchased from Sinopharm Chemical Reagent Co., Ltd. (Beijing, China). All chemicals were directly used without further purification.

2.2. Fabrication of PG Composite Nanofilms. A set of identical graphene dispersions was prepared by liquid exfoliation according to a previous report.[42] In brief, a certain amount of powder was added to 100 mL of DMF or NMP. After sonication in a sonic bath (20 kHz) for 5 h, the dispersions were centrifuged at 3000 rpm for 30 min. The upper dispersion was carefully transferred for further usage. The concentrations of liquid exfoliation graphene dispersions in DMF and NMP are estimated to be 0.08 and 0.1 mg mL^{-1}, respectively. A 200 μL aliquot of PEDOT:PSS aqueous solution was added into the preceding graphene dispersions with a designed ratio, and the resulting mixture was sonicated for 1 h. Finally, the PG nanofilms were prepared by the vacuum filtration of the mixture dispersions onto porous PVDF membrane (0.22 μm). The as-prepared nanofilms were then dried in a vacuum oven at 60 °C for 10 h. For comparison, the pure PEDOT:PSS and graphene nanofilms were fabricated by the same procedure. The PG composite were labeled as PGx (x = 1, 3, 5, 10, 20, 30, 40, 50, 70, and 90) according to the graphene mass percentages in the dried nanofilms.

2.3. Hydrazine Treatment of PG Nanofilms. The HZ-treatment based on the PG3 nanofilm was performed via immersing the nanofilm

DOI: 10.1021/acsami.5b03692
ACS Appl. Mater. Interfaces 2015, 7, 14917−14925

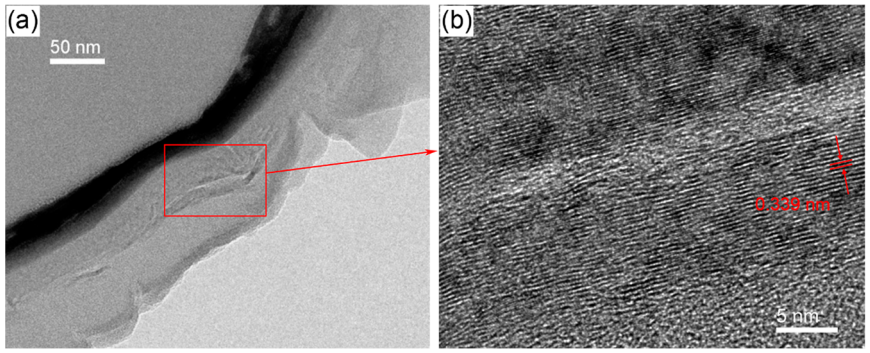

Figure 2. TEM (a) and HRTEM (b) images of graphene films.

in an HZ bath by controlling the HZ concentration, treatment time, and temperature in HZ solution to induce a desired amount of chemical dedoping. Then the dedoped PEDOT:PSS and PG3 nanofilms were rinsed with ethanol and deionized water followed by drying for 5 h at 60 °C under vacuum. The as-prepared PEDOT:PSS and PG3 nanofilms were named PEDOT:PSS-HZ and PG3-HZ, respectively.

2.4. Characterization and Measurement. The surface images and structure of as-prepared nanofilms were obtained by using JEM-2100F (JEOL) high-resolution transmission electron microscopy (TEM) and an atomic force microscope (AFM, Veeco Multimode, Plainview, NY, USA). The thickness of the nanofilms was determined by scanning electron microscopy (SEM) with a dual-beam focused ion beam (FIB, Helios 450S, FEI, Hillsboro, OR, USA) technique. The Raman spectra of the films were collected using a RM2000 (Renishaw, Wotton-under-Edge, U.K.) microscopic confocal Raman spectrometer with argon-ion laser at the excitation wavelength of 514 nm. The surface composition changes of the samples were analyzed using X-ray photoelectron spectroscopy (XPS, Thermo ESCALAB 250Xi, Thermo Scientific, Waltham, MA, USA). UV−vis−near-IR spectra of the samples were taken by using a SPECORD PLUS UV−vis spectrophotometer (Analytik Jena, Jena, Germany). The electrical conductivities of the nanofilms were measured using a standard four-point-probe technique with a Keithley 2700 (Keithley, Cleveland, OH, USA) after four metal lines were patterned with silver paint. The Seebeck coefficient measurements were determined by using Keithley 2700 and 4200 systems (Keithley). The Seebeck coefficient is defined as $S = \Delta V/\Delta T$, where ΔV and ΔT are the voltage drop across the material and the temperature gradient along the voltage. A temperature gradient (5.0 K) was built at ends of films with an ohmic resistance and a Keithley 4200. The ΔV and ΔT were obtained by depositing two Pt100 thermocouples with silver paste on the surface of the films.

3. RESULTS AND DISCUSSION

Figure 1a shows a schematic diagram illustrating the formation process of flexible PG composite nanofilms with use of a vacuum filter method and with HZ posttreatment. As shown in Figure 1b, PEDOT:PSS, PG, and graphene were well-dispersed in DMF. These as-prepared smooth films (Figure 1c) show good flexibility and can be cut to any shape. These properties are superior to those of conventional inorganic TE materials and make the films possible to be applied in flexed or curved energy converters. Figure 2a shows a TEM image of graphene film. The interlayer distance of 0.339 nm (Figure 2b) correspond to the interplanar spacing of the (002) planes of graphene in the insets, which is in good agreement with the previously reported result.[43] The thicknesses of the PEDOT:PSS, PG3, and PG3-HZ nanofilms are 460 ± 42, 575 ± 9.5, and 516 ± 13 nm in Supporting Information Figure S1, respectively.

Figure 3 shows TE properties of PG composite nanofilms as a function of graphene content. The electrical conductivity of

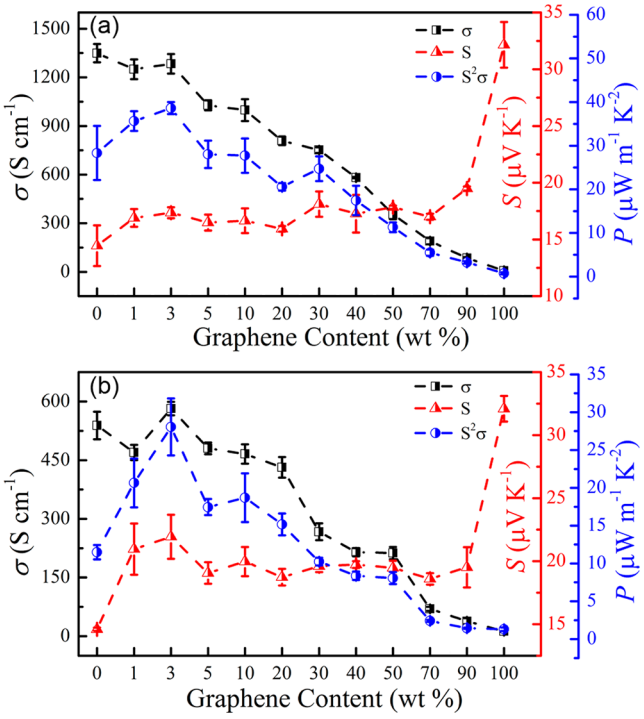

Figure 3. Electrical conductivity, Seebeck coefficient, and power factor of PG composite nanofilms with different contents of graphene in (a) DMF and (b) NMP.

the pure PEDOT:PSS and graphene films prepared in DMF are 1349.4 and 9.2 S cm^{-1} at RT (Figure 3a). As observed, the σ value for the PG nanofilms decreased from 1250 to 85.5 S cm^{-1} with the increasing graphene composition from 1 to 90 wt %. The S value for PG nanofilms increased from 14.6 to 32.3 μV K^{-1} with increasing graphene content up to 100%. Although the increase of the Seebeck coefficient is usually accompanied by the decrease in electrical conductivity,[44] the increase in the Seebeck coefficient is more than the decrease in the electrical conductivity, resulting in an optimized power factor (38.6 μW m^{-1} K^{-2}) for PG nanofilms with 3 wt % graphene prepared in DMF. This behavior could be attributed to two mechanisms: (i) graphene has a higher Seebeck coefficient due to its zero bandgap and a low density of states at the Fermi level;[45] (ii) the strong $\pi-\pi$ interaction between the graphene and conductive PEDOT.[21] When the graphene content is 3 wt %, graphene can

DOI: 10.1021/acsami.5b03692
ACS Appl. Mater. Interfaces 2015, 7, 14917−14925

Table 1. Carrier Concentration (n), Mobility (μ), Calculated Electrical Conductivity (σ_c), and Measured Electrical Conductivity (σ_m) of PEDOT:PSS, Graphene, PG, and PG-HZ Films

samples	graphene content (wt %)	HZ concn ($\times 10^{-3}$ M)	n ($\times 10^{22}$ cm^{-3})	μ (cm^2 V^{-1} s^{-1})	σ_c[a] (S cm^{-1})	σ_m[b] (S cm^{-1})
PEDOT:PSS	0		9.57	0.10	1536	1349
graphene	100		0.04	0.37	24	9.2
PG1	1		7.16	0.11	1260	1250
PG3	3		7.3	0.11	1285	1284
PG10	10		7.0	0.1	1120	998
PG30	30		4.8	0.11	845	752
PG50	50		0.8	0.25	320	355
PG90	90		0.6	0.09	86	86
PG3-HZ-1	3	1	6.0	0.11	1056	1087
PG3-HZ-2	3	5	3.4	0.18	979	1067
PG3-HZ-3	3	20	4.1	0.13	853	928
PG3-HZ-4	3	100	4.6	0.11	810	915
PG3-HZ-5	3	200	4.5	0.11	761	814
PG3-HZ-6	3	400	4.6	0.1	736	800
PG3-HZ-7	3	2000	4.9	0.09	706	735

[a]The calculated electrical conductivity (σ_c) based on $\sigma = ne\mu$; [b]The measured electrical conductivity (σ_m) with a standard four-point-probe technique.

therefore be wrapped by the homogeneous and conductive PEDOT chains leading to a better carrier transport. With the further increase of graphene, the decreasing conductive PEDOT chains are maybe unable to effectively connect to the graphene and decrease the Seebeck coefficient adversely. The PG nanofilms prepared in NMP show similar trends of electrical conductivity and Seebeck coefficient as a function of graphene content (Figure 3b). Moreover, a maximum power factor value (28.0 μW m^{-1} K^{-2}) for PG nanofilms prepared in NMP is also achieved at 3 wt % graphene. This behavior is similar to the PG nanofilms prepared in DMF. In contrast, the PG nanofilms prepared in NMP have a larger Seebeck coefficient but possess a lower electrical conductivity, leading to a lower power factor. This phenomenon may be attributed to DMF, with higher dielectric constants than NMP, inducing a stronger screening effect between counterions and charge carriers, which again reduces the Coulomb interaction between positively charged PEDOT and negatively charged PSS dopants.[46] Therefore, the nanofilms prepared in DMF were used in the subsequent studies.

On the other hand, electrical conductivity is given by[47]

$$\sigma = ne\mu \quad (1)$$

where n is the carrier concentration, e is electron charge, and μ is carrier mobility. The measured electrical conductivities (σ_m) of PEDOT:PSS and PG nanofilms are in good agreement with the calculated values (σ_c) based on eq 1 and recorded in Table 1. Such high electrical conductivity of PEDOT:PSS nanofilm (1394.4 S cm^{-1}) is attributed to a large carrier concentration of pure PEDOT:PSS (9.57×10^{22} cm^{-3}). The PG3 nanofilm has a larger μ value but possesses a lower n value, resulting in a slightly decreased σ value (1283.5 S cm^{-1}) in comparison with that of the PEDOT:PSS nanofilm. Surprisingly, the PG3 nanofilm has a larger power factor (38.6 μW m^{-1} K^{-2}) than the pure PEDOT:PSS nanofilm (28.3 μW m^{-1} K^{-2}) and the previously reported PEDOT:PSS/rGO composite film (11.09 μW m^{-1} K^{-2}).[21] It can be attributed to the following two reasons: (1) the conjugated electron systems of the PEDOT and graphene will interact with each other to provide a channel for carriers transport;[38] (2) exfoliated graphene has much fewer defect sites than rGO, leading to a larger carrier concentration for the PG3 nanofilm.[21] This power factor is lower than that of PEDOT:PSS/SWCNT according to Grunlan et al.[17,18] but higher than that of the reported PEDOT:PSS/SWCNT layered composite films (21.1 μW m^{-1} K^{-2})[20] and PEDOT:PSS/Bi_2Te_3 based alloy nanosheet composite films (32.26 μW m^{-1} K^{-2}).[47]

Further, the PG3 nanofilms were immersed in HZ with different concentrations, treatment times and temperatures. Figure 4a presents the TE properties of the PG3-HZ nanofilms as a function of HZ-treatment concentration for 0.05 min at RT. It can be seen that the electrical conductivity of PG3-HZ nanofilms continuously decreases from 1298 to 783 S cm^{-1} as the HZ concentration increases from 0 to 2.0 M. It is attributed to the fact that dedoping with a high HZ concentration leads to neutral PEDOT with a low concentration of PEDOT. This result is also consistent with the σ_c value as a consequence of eq 1. The Seebeck coefficient of PG3-HZ nanofilms first increased from 17.3 to 23.1 μV K^{-1} with increasing HZ concentration from 0 to 0.1 M and then was almost constant as HZ increased in concentration to 2.0 M. It is well-know that the Seebeck coefficient is correlated to the n value.[44] The decrease of electrical conductivity and the increase of Seebeck coefficient can be rationalized by the decrease of the n value for PG3 by HZ-treatment (Table 1), which is in good agreement with the previous report.[48] We obtained a maximum power factor of 53.3 μW m^{-1} K^{-2} at 5×10^{-3} M, which is 1.9 times larger than that of the pure PEDOT:PSS nanofilm (28.3 μW m^{-1} K^{-2}).

The effects of HZ (5×10^{-3} M) treatment time on the σ and S of PG3-HZ nanofilms were investigated in Figure 4b. It can be seen that the electrical conductivity of the PG3-HZ nanofilms decreases dramatically from 1283.5 to 641 S cm^{-1} as the treatment time delays, while Seebeck coefficient reached the highest value (22.5 μV K^{-1}) at 0.05 min and then fluctuated within a small range, resulting in a peak power factor value (53.3 μW m^{-1} K^{-2}) after treatment for 0.05 min. Figure 4c shows the TE properties of the PG3-HZ nanofilms as a function of HZ-treatment (5×10^{-3} M) temperature. With increasing HZ-treatment temperature from RT to 100 °C, the electrical conductivity for PG3-HZ nanofilms decreased dramatically from 1067 to 647 S cm^{-1}. When the treatment temperature is higher than 60 °C, the Seebeck coefficient remains generally stable at ~23 μV K^{-1} for PG3-HZ nanofilms. Hence, the power factor for PG3-HZ nanofilms decreased with

DOI: 10.1021/acsami.5b03692
ACS Appl. Mater. Interfaces 2015, 7, 14917−14925

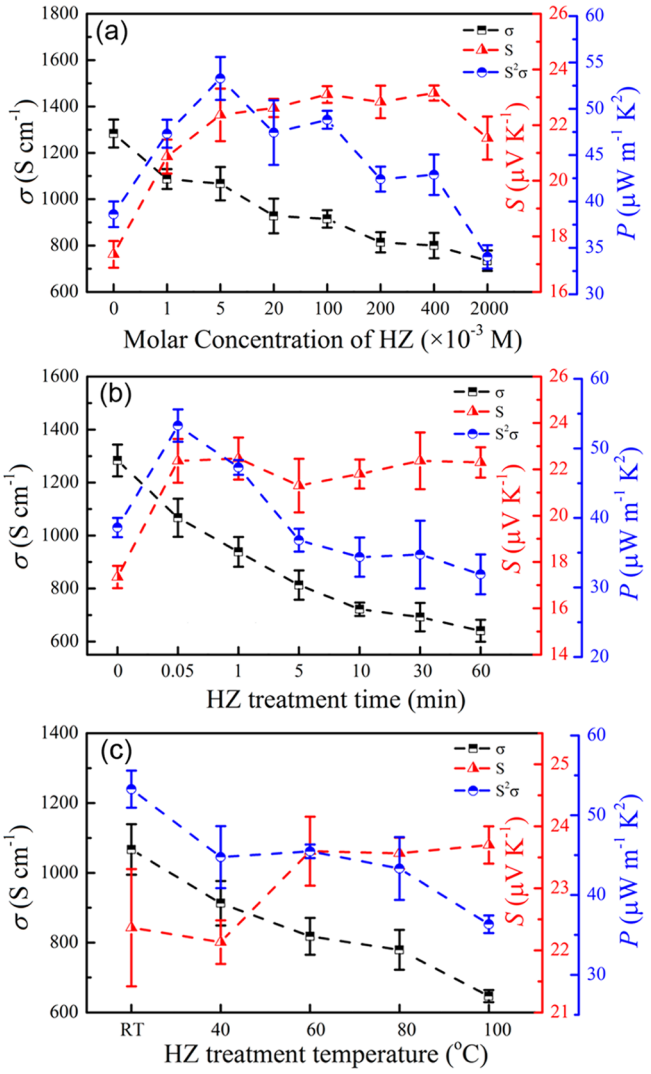

Figure 4. TE properties of PG3-HZ nanofilms as a function of (a) HZ concentration dipping for 0.05 min at RT, (b) HZ (5×10^{-3} M) treatment time at RT, and (c) HZ (5×10^{-3} M) treatment temperature dipping for 0.05 min.

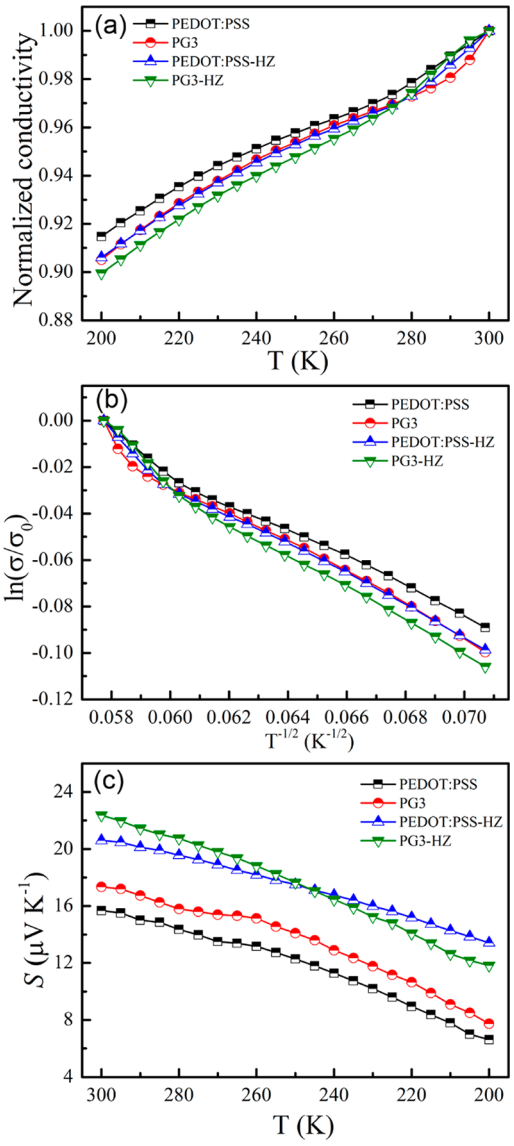

Figure 5. (a) Temperature dependences of the normalized electrical conductivity of PEDOT:PSS and PG3 before and after HZ-treatment. (b) Analyses of the temperature dependences of the electrical conductivity with the 1D VRH model. (c) Temperature dependences of the Seebeck coefficient of PEDOT:PSS and PG3 before and after HZ-treatment. The electrical conductivities are normalized to those of the corresponding samples at 300 K (i.e., σ_0 is the electrical conductivity at 300 K).

increasing temperature of HZ-treatment, thus resulting in a maximum value of 53.3 μW m^{-1} K^{-2} at RT. This was mainly due to the considerably decreased electrical conductivity and little variation for the Seebeck coefficient. According to the reported thermal conductivity in the through-plane of 3 wt % rGO in PEDOT:PSS (0.3 W m^{-1} K^{-1}),[21] an estimated maximum ZT value of 0.05 can be achieved with 5×10^{-3} M HZ-treatment for 0.05 min at RT.

The electrical conductivity is investigated from 300 down to 200 K for as-prepared nanofilms to understand the conduction mechanism. As shown in Figure 5a, the electrical conductivity increases with the increasing temperature, suggesting that these samples are semiconductor materials. The relationship between electrical conductivity and temperature can be fitted by the one-dimensional variable range-hopping (VRH) mechanism[10,46]

$$\sigma(T) = \sigma_0 \exp\left[\left(\frac{T_0}{T}\right)^{1/2}\right] \quad (2)$$

where σ_0 is a constant and T_0 is the energy barrier between localized states. The T_0 values of the PEDOT:PSS, PG3, PEDOT:PSS-HZ, and PG3-HZ nanofilms are estimated to be 39.1, 46.8, 51.3, and 55.4 K based on Figure 5b, respectively. It is noted that the increasing T_0 can be found for nanofilms after HZ-treatment, indicating the increasing carrier hopping barrier. Thus, HZ-treatment can enhance the energy barrier for the interchain and interdomain charge hopping, leading to a decreasing electrical conductivity. Additionally, the Seebeck coefficient of as-prepared nanofilms also decreased with the decreasing temperature (Figure 5c), and the same behavior was observed for the electrical conductivity.

To explore the effects of the surface chemical compositions of as-prepared films on electrical conductivity and Seebeck coefficient, the X-ray photoelectron spectroscopy (XPS) survey spectra were analyzed, as shown in Figure 6. The S_{2p} peaks at 166 and 172 eV originate from the sulfur atoms of PSS, and the

DOI: 10.1021/acsami.5b03692
ACS Appl. Mater. Interfaces 2015, 7, 14917−14925

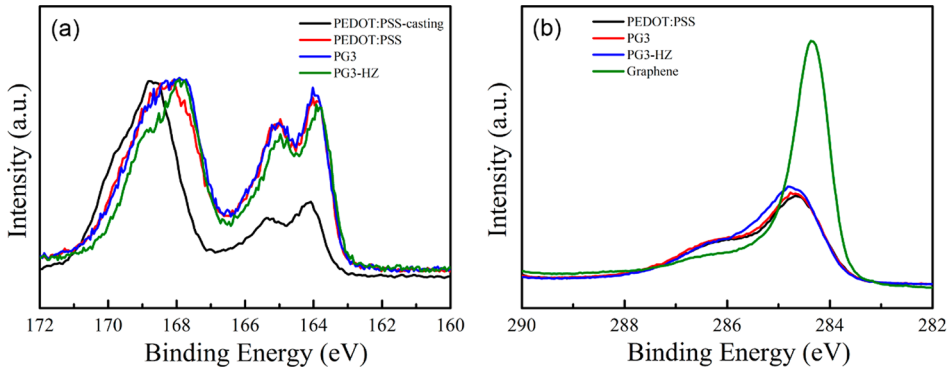

Figure 6. X-ray photoelectron spectroscopy (XPS) analysis of PEDOT:PSS-casting, PEDOT:PSS, graphene, PG3, and PG3-HZ films: (a) S_{2p} spectra and (b) C_{1s} spectra.

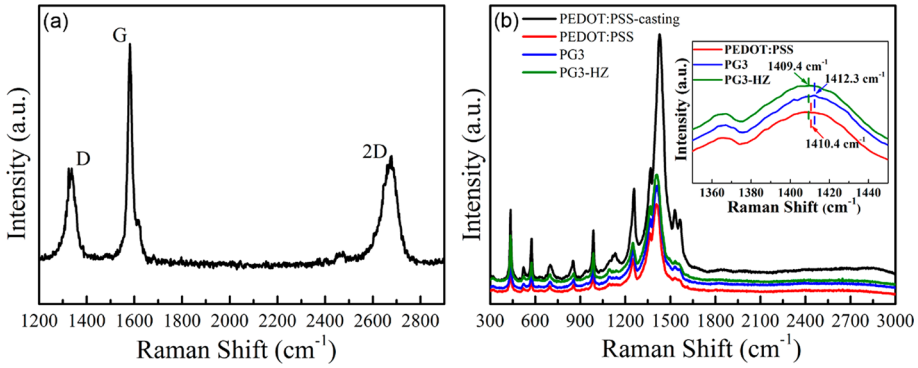

Figure 7. Raman spectra of (a) graphene and (b) PEDOT:PSS-casting, PEDOT:PSS, PG3, and PG3-HZ films.

two XPS bands with the binding energies between 162 and 166 eV being due to the sulfur atoms of PEDOT in Figure 6a.[8,49] Compared to PEDOT:PSS-casting film (pristine PEDOT:PSS film prepared by casting is henceforth denoted as PEDOT:PSS-casting), the S_{2p} XPS intensity ratio of PEDOT to PSS increases for the nanofilms prepared by vacuum filtration. In addition, there was no significant change for the S_{2p} peak intensity ratio of PEDOT to PSS among these nanofilms of vacuum filtration. These results suggest that some PSS chains in DMF were away from the surface region of the PEDOT:PSS film during the film-forming process, which can lead a conformational change between PEDOT and PSS chains.[41,50] Therefore, a thin layer of high electrical conductivity with high PEDOT concentration is formed on the surface of the film.[51] In comparison with PEDOT:PSS and PG3, the peaks of PG3-HZ for PSS are shifted to slightly lower binding energy, indicating that the sulfonic acid groups ($-SO_3^-H^+$) interacted with HZ to form the complex ($-SO_3^-N_2H_5^+$). A similar low-energy shift of PG3 after a HZ-treatment in PEDOT is also observed, suggesting that the electrostatic interaction between the PEDOT and PSS units might be weaker due to the presence of HZ between PEDOT and PSS.[52] The main peak in the C_{1s} spectra of graphene film is fitted with two peaks at 284.35 and 286.67 eV, which are associated with C−C and C−O, respectively (Figure 6b). Typical carbon bonds in the PEDOT:PSS were observed at ~284.64 (C−C/C−H), ~285.44 (C−S), ~286.64 (C═C−O), and ~287.79 eV (C−O−C), respectively, which is in good agreement with the previous report.[23,53] The PG3 peaks are shifted about 0.05 eV toward higher binding energy levels compared to PEDOT:PSS, due to the electron donation of PEDOT:PSS through the strong $\pi-\pi$ interaction between PEDOT:PSS and the graphene surface.[54] A similar energy shift to a higher level of the C_{1s} spectra after the HZ-treatment for the PG3 nanofilm has also been observed, which implies that the additional electrons brought by HZ lead to a blue shift in the Fermi level.[55] These results suggest that the loss of PSS from PEDOT:PSS after vacuum filtration and a channel for carrier transport can be provided after composite and HZ-treatment, resulting in a decreasing σ value and an increasing S value for PG3-HZ nanofilms.

Figure 7 gives the Raman spectra of graphene, PEDOT:PSS-casting, PEDOT:PSS, PG3, and PG3-HZ films. Figure 7a shows the typical Raman spectra of exfoliated graphene. The band between 1400 and 1500 cm^{-1} is due to C═C symmetric stretching vibration (Figure 7b). The peak at 1429.17 cm^{-1} for the PEDOT:PSS-casting film is red-shifted to 1410.40 cm^{-1} compared to the PEDOT:PSS nanofilm due to the effects of size-induced phonon confinement and surface relaxation.[56] Moreover, the bands at 1570 cm^{-1} correspond to the C═C antisymmetric stretching, at 1365 cm^{-1} to the single C−C stretching, at 1262 cm^{-1} to the C−C interring stretching, and at 990 cm^{-1} to the deformations of oxyethylene ring.[57,58] Compared to the spectrum of PEDOT:PSS, the peaks of PG3 at 1410.1 cm^{-1} are slightly shifted to a higher wavenumber of 1412.3 cm^{-1}, indicting strong $\pi-\pi$ interaction of aromatic structures of PEDOT:PSS and electron-rich graphene.[21,23] Additionally, the HZ-treatment leads to a slight red shift of C═C from 1412.3 to 1409.4 cm^{-1}, suggesting the decrease in the doping level from bipolaron to polaron or neutral invariably.[48,53] This result is consistent with the UV−vis−near-IR absorption spectra (Supporting Information Figure S2) and the measured carrier concentration value in Table 1.

DOI: 10.1021/acsami.5b03692
ACS Appl. Mater. Interfaces 2015, 7, 14917−14925

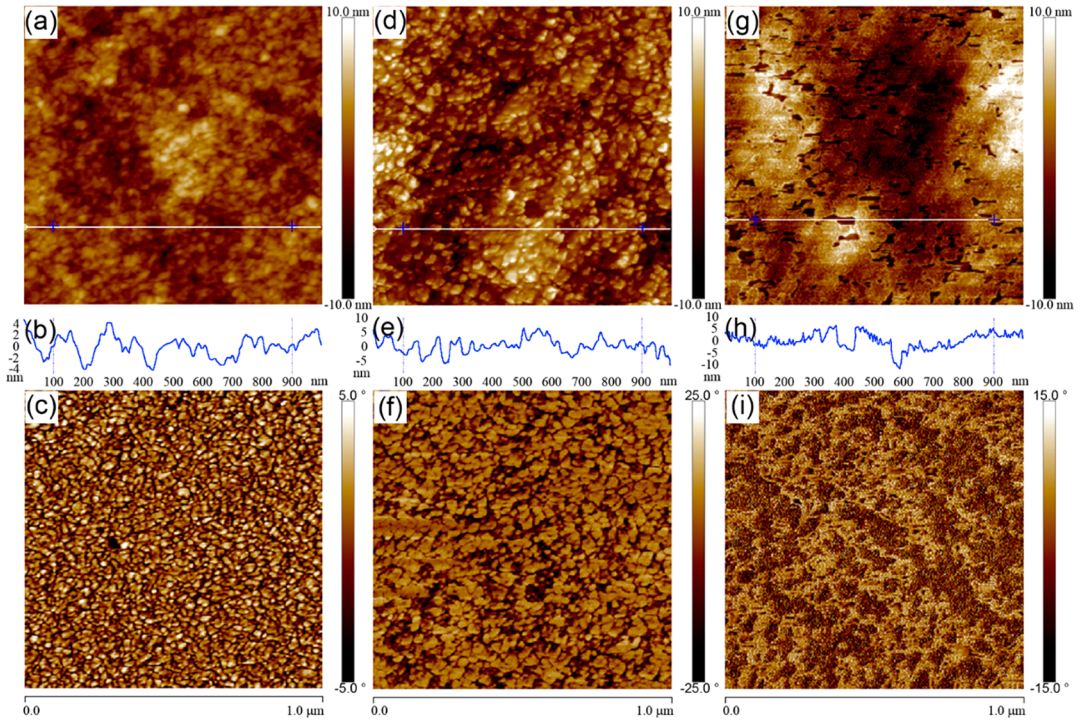

Figure 8. AFM images of the samples. (a) PEDOT:PSS, (d) PG3, and (g) PG3-HZ are height images. Panels b, e, and h are height profiles corresponding to a, d, and g, respectively. Panels c, f, and I are phase images corresponding to a, d, and g, respectively. All of the images are 1 μm × 1 μm.

Figure 8 presents the AFM images of PEDOT:PSS, PG3, and PG3-HZ nanofilms to investigate possible changes in the surface morphology. In the phase image for PEDOT:PSS nanofilm (Figure 8c), the bright (positive) and dark (negative) phase shifts correspond to PEDOT-rich grains and PSS-rich grains, respectively, which shows better phase separation between PEDOT and PSS chains with more fiber such as interconnected conductive PEDOT chains.[59,60] The PG3 nanofilm has a rougher surface compared to the PEDOT:PSS nanofilm, and the graphene can be seen clearly in the PEDOT:PSS matrix (Figure 8f). Note that the aggregated nanoparticles on PG3-HZ are more visible compared with PG3, suggesting that a large portion of the PSS-rich regions was removed after the HZ-treatment (Figure 8l). Furthermore, the height images and profiles show that the average roughness (R_a) is 1.60, 2.38, and 3.26 nm for PEDOT:PSS, PG3, and PG3-HZ nanofilms, respectively. This morphologic change suggests the conformational change between PEDOT and PSS chains after HZ-treatment, and the PG3-HZ nanofilms have a much longer polymer chain than PEDOT:PSS and PG3 nanofilms.

4. CONCLUSIONS

In summary, we have successfully fabricated flexible PG composite nanofilms with liquid exfoliated graphene and PEDOT:PSS solution by a direct vacuum filtration. The PG nanofilm achieved a larger TE power factor of 38.6 μW m^{-1} K^{-2} with 3 wt % graphene than that of pure PEDOT:PSS nanofilm due to the high electrical conductivity (1283.5 S cm^{-1}) and the enhanced Seebeck coefficient (22.0 μV K^{-1}). The most important contribution of graphene is to improve the Seebeck coefficient of pristine PEDOT:PSS. This behavior is attributed to the fact that the conjugated electron systems of the graphene can interact with PEDOT:PSS to provide a channel for carrier transport. Further, we found that HZ-treatment has a positive effect on the improvement of the Seebeck coefficient for PG3 nanofilm despite a decreasing electrical conductivity. An optimized power factor of 53.3 μW m^{-1} K^{-2} is achieved for PG3 nanofilm by adjusting hydrazine concentration, treatment time, and temperature. Assuming a thermal conductivity of 0.3 W m^{-1} K^{-1} in a through-plane direction, the corresponding ZT is estimated to be 0.05 at room temperature, which are higher than previous reports of PEDOT:PSS/rGO films.

■ ASSOCIATED CONTENT

Supporting Information

Cross-section SEM images for samples showing thin-film thickness for as-prepared films and UV−vis−near-IR absorption spectra of PG3-HZ nanofilms as a function of HZ concentration. The Supporting Information is available free of charge on the ACS Publications website at DOI: 10.1021/acsami.5b03692.

■ AUTHOR INFORMATION

Corresponding Author

*Tel.: +86-791-88537967. Fax: +86-791-83823320. E-mail: xujingkun@tsinghua.org.cn.

Author Contributions

†J.H. Xiong and F.X. Jiang contributed equally to this work.

Notes

The authors declare no competing financial interest.

■ ACKNOWLEDGMENTS

We gratefully acknowledge the financial support of the National Natural Science Foundation of China (Grant Nos. 51463008 and 51402134), the Ganpo Outstanding Talents 555 projects,

DOI: 10.1021/acsami.5b03692
ACS Appl. Mater. Interfaces 2015, 7, 14917−14925

and the Youth Outstanding Talent Project of Jiangxi Science and Technology Normal University.

REFERENCES

(1) Kim, G. H.; Shao, L.; Zhang, K.; Pipe, K. P. Engineered Doping of Organic Semiconductors for Enhanced Thermoelectric Efficiency. *Nat. Mater.* **2013**, *12*, 719−723.
(2) Bubnova, O.; Khan, Z. U.; Malti, A.; Braun, S.; Fahlman, M.; Berggren, M.; Crispin, X. Optimization of the Thermoelectric Figure of Merit in the Conducting Polymer Poly(3,4-ethylenedioxythiophene). *Nat. Mater.* **2011**, *10*, 429−433.
(3) Jiang, F. X.; Xu, J. K.; Lu, B. Y.; Xie, Y.; Huang, R. J.; Li, L. F. Thermoelectric Performance of Poly(3,4-ethylenedioxythiophene):Poly(styrenesulfonate). *Chin. Phys. Lett.* **2008**, *25*, 2202−2205.
(4) Du, Y.; Shen, S. Z.; Cai, K.; Casey, P. S. Research Progress on Polymer−Inorganic Thermoelectric Nanocomposite Materials. *Prog. Polym. Sci.* **2012**, *37*, 820−841.
(5) Abad, B.; Alda, I.; Díaz-Chao, P.; Kawakami, H.; Almarza, A.; Amantia, D.; Gutierrez, D.; Aubouy, L.; Martín-González, M. Improved Power Factor of Polyaniline Nanocomposites with Exfoliated Graphene Nanoplatelets (GNPs). *J. Mater. Chem. A* **2013**, *1*, 10450−10457.
(6) Yue, R.; Xu, J. Poly(3,4-ethylenedioxythiophene) as Promising Organic Thermoelectric Materials: A Mini-Review. *Synth. Met.* **2012**, *162*, 912−917.
(7) Kong, F. F.; Liu, C. C.; Xu, J. K.; Jiang, F. X.; Lu, B. Y.; Yue, R. R.; Liu, G. D.; Wang, J. M. Simultaneous Enhancement of Electrical Conductivity and Seebeck Coefficient of Poly(3,4-ethylenedioxythiophene):Poly(styrenesulfonate) Films Treated with Urea. *Chin. Phys. Lett.* **2011**, *28*, No. 037201.
(8) Xia, Y.; Ouyang, J. Significant Conductivity Enhancement of Conductive Poly(3,4-ethylenedioxythiophene):Poly(styrenesulfonate) Films through a Treatment with Organic Carboxylic Acids and Inorganic Acids. *ACS Appl. Mater. Interfaces* **2010**, *2*, 474−483.
(9) Ouyang, J.; Chu, W. C.; Chen, F. C.; Xu, Q.; Yang, Y. High-Conductivity Poly(3,4-ethylenedioxythiophene):Poly(styene sulfonate) Film and Its Application in Polymer Optoelectronic Devices. *Adv. Funct. Mater.* **2005**, *15*, 203−208.
(10) Yao, Q.; Chen, L.; Zhang, W.; Liufu, S.; Chen, X. Enhanced Thermoelectric Performance of Single-Walled Carbon Nanotubes/Polyaniline Hybrid Nanocomposites. *ACS Nano* **2010**, *4*, 2445−2451.
(11) Mengistie, D. A.; Chen, C.; Boopathi, K. M.; Pranoto, F. W.; Li, L.; Chu, C. Enhanced Thermoelectric Performance of PEDOT:PSS Flexible Bulky Papers by Treatment with Secondary Dopants. *ACS Appl. Mater. Interfaces* **2015**, *7*, 94−100.
(12) Xia, Y.; Sun, K.; Ouyang, J. Solution-Processed Metallic Conducting Polymer Films as Transparent Electrode of Optoelectronic Devices. *Adv. Mater.* **2012**, *24*, 2436−2440.
(13) He, M.; Qiu, F.; Lin, Z. Towards High-Performance Polymer-Based Thermoelectric Materials. *Energy Environ. Sci.* **2013**, *6*, 1352−1361.
(14) See, K. C.; Feser, J. P.; Chen, C. E.; Majumdar, A.; Urban, J. J.; Segalman, R. A. Water-Processable Polymer-Nanocrystal Hybrids for Thermoelectrics. *Nano Lett.* **2010**, *10*, 4664−4667.
(15) Zhang, B.; Sun, J.; Katz, H. E.; Fang, F.; Opila, R. L. Promising Thermoelectric Properties of Commercial PEDOT:PSS Materials and Their Bi_2Te_3 Powder Composites. *ACS Appl. Mater. Interfaces* **2010**, *2*, 3170−3178.
(16) Park, G. O.; Roh, J. W.; Kim, J.; Lee, K. Y.; Jang, B.; Lee, K. H.; Lee, W. Enhanced Thermoelectric Properties of Germanium Powder/Poly(3,4-ethylenedioxythiophene):Poly(4-styrenesulfonate) Composites. *Thin Solid Films* **2014**, *566*, 14−18.
(17) Moriarty, G. P.; Briggs, K.; Stevens, B.; Yu, C.; Grunlan, J. C. Fully Organic Nanocomposites with High Thermoelectric Power Factors by Using a Dual-Stabilizer Preparation. *Energy Technol.* **2013**, *1*, 265−272.
(18) Yu, C.; Choi, K.; Yin, L.; Grunlan, J. C. Light-Weight Flexible Carbon Nanotube Based Organic Composites with Large Thermoelectric Power Factors. *ACS Nano* **2011**, *5*, 7885−7892.
(19) Kim, D.; Kim, Y.; Choi, K.; Grunlan, J. C.; Yu, C. Improved Thermoelectric Behavior of Nanotube-Filled Polymer Composites with Poly(3,4-ethylenedioxythiophene):Poly(styrenesulfonate). *ACS Nano* **2010**, *4*, 513−523.
(20) Song, H.; Liu, C.; Xu, J.; Jiang, Q.; Shi, H. Fabrication of a Layered Nanostructure PEDOT:PSS/SWCNTs Composite and Its Thermoelectric Performance. *RSC Adv.* **2013**, *3*, 22065−22071.
(21) Kim, G. H.; Hwang, D. H.; Woo, S. I. Thermoelectric Properties of Nanocomposite Thin Films Prepared with Poly(3,4-ethylenedioxythiophene) Poly(styrenesulfonate) and Graphene. *Phys. Chem. Chem. Phys.* **2012**, *14*, 3530−3536.
(22) Li, F.; Cai, K.; Shen, S.; Chen, S. Preparation and Thermoelectric Properties of Reduced Graphene Oxide/PEDOT:PSS Composite Films. *Synth. Met.* **2014**, *197*, 58−61.
(23) Yoo, D.; Kim, J.; Kim, J. H. Direct Synthesis of Highly Conductive Poly(3,4-ethylenedioxythiophene):Poly(4-styrenesulfonate) (PEDOT:PSS)/Graphene Composites and Their Applications in Energy Harvesting Systems. *Nano Res.* **2014**, *7*, 717−730.
(24) Zhu, Y.; Murali, S.; Stoller, M. D.; Velamakanni, A.; Piner, R. D.; Ruoff, R. S. Microwave Assisted Exfoliation and Reduction of Graphite Oxide for Ultracapacitors. *Carbon* **2010**, *48*, 2106−2122.
(25) Bolotin, K. I.; Sikes, K. J.; Jiang, Z.; Klima, M.; Fudenberg, G.; Hone, J.; Kim, P.; Stormer, H. L. Ultrahigh Electron Mobility in Suspended Graphene. *Solid State Commun.* **2008**, *146*, 351−355.
(26) Lotya, M.; Hernandez, Y.; King, P. J.; Smith, R. J.; Nicolosi, V.; Karlsson, L. S.; Blighe, F. M.; De, S.; Wang, Z.; McGovern, I. T.; Duesberg, G. S.; Coleman, J. N. Liquid Phase Production of Graphene by Exfoliation of Graphite in Surfactant/Water Solutions. *J. Am. Chem. Soc.* **2009**, *131*, 3611−3620.
(27) Jin, Z.; Lomeda, J. R.; Price, B. K.; Lu, W.; Zhu, Y.; Tour, J. M. Mechanically Assisted Exfoliation and Functionalization of Thermally Converted Graphene Sheets. *Chem. Mater.* **2009**, *21*, 3045−3047.
(28) Cai, M.; Thorpe, D.; Adamson, D. H.; Schniepp, H. C. Methods of Graphite Exfoliation. *J. Mater. Chem.* **2012**, *22*, 24992−25002.
(29) Guardia, L.; Fernández-Merino, M. J.; Paredes, J. I.; Solís-Fernández, P.; Villar-Rodil, S.; Martínez-Alonso, A.; Tascón, J. M. D. High-Throughput Production of Pristine Graphene in an Aqueous Dispersion Assisted by Non-ionic Surfactants. *Carbon* **2011**, *49*, 1653−1662.
(30) Ni, X.; Liang, G.; Wang, J.-S.; Li, B. Disorder Enhances Thermoelectric Figure of Merit in Armchair Graphane Nanoribbons. *Appl. Phys. Lett.* **2009**, *95*, No. 192114.
(31) Xu, Y.; Li, Z.; Duan, W. Thermal and Thermoelectric Properties of Graphene. *Small* **2014**, *10*, 2182−2199.
(32) Zuev, Y.; Chang, W.; Kim, P. Thermoelectric and Magnetothermoelectric Transport Measurements of Graphene. *Phys. Rev. Lett.* **2009**, *102*, No. 096807.
(33) Wang, C. R.; Lu, W. S.; Hao, L.; Lee, W. L.; Lee, T. K.; Lin, F.; Cheng, I. C.; Chen, J. Z. Enhanced Thermoelectric Power in Dual-Gated Bilayer Graphene. *Phys. Rev. Lett.* **2011**, *107*, No. 186602.
(34) Ghosh, S.; Calizo, I.; Teweldebrhan, D.; Pokatilov, E. P.; Nika, D. L.; Balandin, A. A.; Bao, W.; Miao, F.; Lau, C. N. Extremely High Thermal Conductivity of Graphene: Prospects for Thermal Management Applications in Nanoelectronic Circuits. *Appl. Phys. Lett.* **2008**, *92*, No. 151911.
(35) Lin, J.; Teweldebrhan, D.; Ashraf, K.; Liu, G.; Jing, X.; Yan, Z.; Li, R.; Ozkan, M.; Lake, R. K.; Balandin, A. A.; Ozkan, C. S. Gating of Single-Layer Graphene with Single-Stranded Deoxyribonucleic Acids. *Small* **2010**, *6*, 1150−1155.
(36) Hong, W.; Xu, Y.; Lu, G.; Li, C.; Shi, G. Transparent Graphene/PEDOT−PSS Composite Films as Counter Electrodes of Dye-Sensitized Solar Cells. *Electrochem. Commun.* **2008**, *10*, 1555−1558.
(37) Zhang, M.; Yuan, W.; Yao, B.; Li, C.; Shi, G. Solution-Processed PEDOT:PSS/Graphene Composites as the Electrocatalyst for Oxygen Reduction Reaction. *ACS Appl. Mater. Interfaces* **2014**, *6*, 3587−3593.

DOI: 10.1021/acsami.5b03692
ACS Appl. Mater. Interfaces 2015, 7, 14917−14925

(38) Seol, Y. G.; Trung, T. Q.; Yoon, O. J.; Sohn, I. Y.; Lee, N. E. Nanocomposites of Reduced Graphene Oxide Nanosheets and Conducting Polymer for Stretchable Transparent Conducting Electrodes. *J. Mater. Chem.* **2012**, *22*, 23759−23766.
(39) Stankovich, S.; Dikin, D. A.; Piner, R. D.; Kohlhaas, K. A.; Kleinhammes, A.; Jia, Y.; Wu, Y.; Nguyen, S. T.; Ruoff, R. S. Synthesis of Graphene-Based Nanosheets via Chemical Reduction of Exfoliated Graphite Oxide. *Carbon* **2007**, *45*, 1558−1565.
(40) Khan, U.; O'Neill, A.; Lotya, M.; De, S.; Coleman, J. N. High-Concentration Solvent Exfoliation of Graphene. *Small* **2010**, *6*, 864−871.
(41) Ouyang, J.; Xu, Q.; Chu, C.-W.; Yang, Y.; Li, G.; Shinar, J. On the Mechanism of Conductivity Enhancement in Poly(3,4-ethylenedioxythiophene):Poly(styrene sulfonate) Film Through Solvent Treatment. *Polymer* **2004**, *45*, 8443−8450.
(42) Coleman, J. N.; Lotya, M.; O'Neill, A.; Bergin, S. D.; King, P. J.; Khan, U.; Young, K.; Gaucher, A.; De, S.; Smith, R. J.; Shvets, I. V.; Arora, S. K.; Stanton, G.; Kim, H. Y.; Lee, K.; Kim, G. T.; Duesberg, G. S.; Hallam, T.; Boland, J. J.; Wang, J. J.; Donegan, J. F.; Grunlan, J. C.; Moriarty, G.; Shmeliov, A.; Nicholls, R. J.; Perkins, J. M.; Grieveson, E. M.; Theuwissen, K.; McComb, D. W.; Nellist, P. D.; Nicolosi, V. Two-Dimensional Nanosheets Produced by Liquid Exfoliation of Layered Materials. *Science* **2011**, *331*, 568−571.
(43) Zheng, J.; Liu, H.; Wu, B.; Guo, Y.; Wu, T.; Yu, G.; Liu, Y.; Zhu, D. Production of Graphene Nanospheres by Annealing of Graphene Oxide in Solution. *Nano Res.* **2011**, *4*, 705−711.
(44) Tsai, T. C.; Chang, H. C.; Chen, C. H.; Whang, W. T. Widely Variable Seebeck Coefficient and Enhanced Thermoelectric Power of PEDOT:PSS Films by Blending Thermal Decomposable Ammonium Formate. *Org. Electron.* **2011**, *12*, 2159−2164.
(45) Bubnova, O.; Khan, Z. U.; Wang, H.; Braun, S.; Evans, D. R.; Fabretto, M.; Hojati-Talemi, P.; Dagnelund, D.; Arlin, J. B.; Geerts, Y. H.; Desbief, S.; Breiby, D. W.; Andreasen, J. W.; Lazzaroni, R.; Chen, W. M.; Zozoulenko, I.; Fahlman, M.; Murphy, P. J.; Berggren, M.; Crispin, X. Semi-Metallic Polymers. *Nat. Mater.* **2014**, *13*, 190−194.
(46) Kim, J. Y.; Jung, H. J.; Lee, D. E.; Joo, J. Enhancement of Electrical Conductivity of Poly(3,4-ethylenedioxythiophene)/Poly(4-styrenesulfonate) by a Change of Solvents. *Synth. Met.* **2002**, *126*, 311−316.
(47) Du, Y.; Cai, K. F.; Chen, S.; Cizek, P.; Lin, T. Facile Preparation and Thermoelectric Properties of Bi_2Te_3 Based Alloy Nanosheet/PEDOT:PSS Composite Films. *ACS Appl. Mater. Interfaces* **2014**, *6*, 5735−5743.
(48) Park, H.; Lee, S. H.; Kim, F. S.; Choi, H. H.; Cheong, I. W.; Kim, J. H. Enhanced Thermoelectric Properties of PEDOT:PSS Nanofilms by a Chemical Dedoping Process. *J. Mater. Chem. A* **2014**, *2*, 6532−6539.
(49) Ouyang, J. Solution-Processed PEDOT:PSS Films with Conductivities as Indium Tin Oxide through a Treatment with Mild and Weak Organic Acids. *ACS Appl. Mater. Interfaces* **2013**, *5*, 13082−13088.
(50) Xia, Y.; Ouyang, J. Salt-Induced Charge Screening and Significant Conductivity Enhancement of Conducting Poly(3,4-ethylenedioxythiophene):Poly(styrenesulfonate). *Macromolecules* **2009**, *42*, 4141−4147.
(51) Jönsson, S. K. M.; Birgerson, J.; Crispin, X.; Greczynski, G.; Osikowicz, W.; Denier van der Gon, A. W.; Salaneck, W. R.; Fahlman, M. The Effects of Solvents on the Morphology and Sheet Resistance in Poly(3,4-ethylenedioxythiophene)−Polystyrenesulfonic Acid (PEDOT−PSS) Films. *Synth. Met.* **2003**, *139*, 1−10.
(52) Hwang, J.; Amy, F.; Kahn, A. Spectroscopic Study on Sputtered PEDOT·PSS: Role of Surface PSS Layer. *Org. Electron.* **2006**, *7*, 387−396.
(53) Armes, M. A.; Armes, S. P. Surface Characterization of Poly(3,4-ethylenedioxythiophene)-Coated Latexes by X-ray Photoelectron Spectroscopy. *Langmuir* **2000**, *16*, 4171−4179.
(54) Su, Q.; Pang, S.; Alijani, V.; Li, C.; Feng, X.; Müllen, K. Composites of Graphene with Large Aromatic Molecules. *Adv. Mater.* **2009**, *21*, 3191−3195.
(55) Graupner, R.; Abraham, J.; Vencelov, A.; Seyller, T.; Hennrich, F.; Kappes, M. M.; Hirsch, A.; Ley, L. Doping of Single-Walled Carbon Nanotube Bundles by Brønsted Acids. *Phys. Chem. Chem. Phys.* **2003**, *5*, 5472−5476.
(56) Yang, C. C.; Li, S. Size-Dependent Raman Red Shifts of Semiconductor Nanocrystals. *J. Phys. Chem. B* **2008**, *112*, 14193−14197.
(57) Wang, J.; Cai, K.; Shen, S. Enhanced Thermoelectric Properties of Poly(3,4-ethylenedioxythiophene) Thin Films Treated with H_2SO_4. *Org. Electron.* **2014**, *15*, 3087−3095.
(58) Garreau, S.; Louarn, G.; Buisson, J. P.; Froyer, G.; Lefrant, S. In Situ Spectroelectrochemical Raman Studies of Poly(3,4-ethylenedioxythiophene) (PEDT). *Macromolecules* **1999**, *32*, 6807−6812.
(59) Lang, U.; Müller, E.; Naujoks, N.; Dual, J. Microscopical Investigations of PEDOT:PSS Thin Films. *Adv. Funct. Mater.* **2009**, *19*, 1215−1220.
(60) Mengistie, D. A.; Ibrahem, M. A.; Wang, P. C.; Chu, C. W. Highly Conductive PEDOT:PSS Treated with Formic Acid for ITO-Free Polymer Solar Cells. *ACS Appl. Mater. Interfaces* **2014**, *6*, 2292−2299.

DOI: 10.1021/acsami.5b03692
ACS Appl. Mater. Interfaces 2015, 7, 14917−14925